JIM / TMS Solidification Science and Processing Conference, Honolulu, HI, Dec. 13-15, 1995. pp. 197-208.

THERMAL DISTORTION OF SOLIDIFYING SHELL NEAR MENISCUS IN CONTINUOUS CASTING OF STEEL

B. G. Thomas and H. Zhu

Department of Mechanical and Industrial Engineering
University of Illinois at Urbana-Champaign
1206 West Green Street
Urbana, IL 61801

Abstract

A two-dimensional, transient, finite-element model has been developed to simulate temperature, shape, and stress development in the steel shell, during the initial stages of solidification in the mold. The model is applied to predict the distorted shape of a vertical section through the shell, during a sudden fluctuation in liquid level at the meniscus. The calculation includes the effects of temperature-dependent properties, thermal shrinkage, phase transformations, and creep, using an elastic-viscoplastic constitutive equation for low carbon steel. The model features a robust, efficient algorithm to integrate the highly temperature- and stress-dependent constitutive equation for the inelastic-creep strain rate. The results show that thermal stress causes the exposed portion of the thin shell to bend towards the liquid, when there is a sudden drop in liquid level. In addition, the axial temperature gradient creates high transverse stresses. The subsequent rise in liquid level increases the bending. These results illustrate an important mechanism contributing to the formation of transverse surface depressions and short longitudinal surface cracks associated with liquid level fluctuations.

Introduction

Most of the surface defects in continuous casting are suspected to initiate during the early stages of solidification in the mold, especially near the meniscus pictured in Figure 1. These defects include deep oscillation marks, surface depressions, longitudinal and transverse surface cracks. Although a body of empirical knowledge and evidence exists, the exact mechanisms for many of these problems are still unclear.

Undoubtedly, there are several different causes of different types of surface depressions. Oscillation marks have been proposed to originate from pressure buildup in the lubricating flux channel between the shell tip and mold during the negative strip time. [1] Interaction between the initial shell and the solid flux rim, [2] or negative taper of the mold wall in the meniscus region [3] has been proposed to further add to this mechanism. Alternatively, if the meniscus freezes, this leads to a "meniscus mark" depression, often beneath a subsurface "hook", [1] when the liquid steel level overflows the meniscus each oscillation cycle. [4]

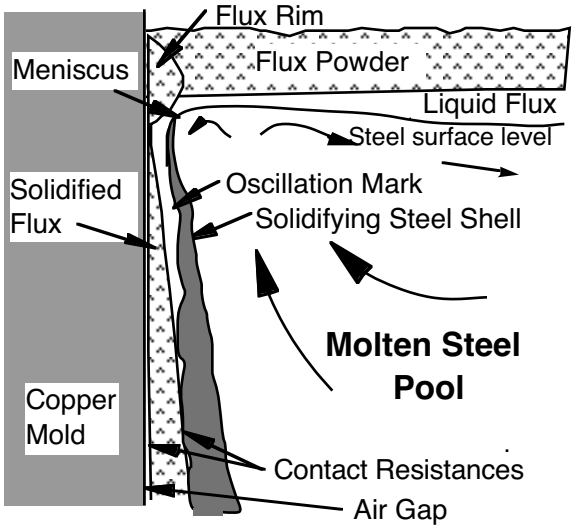

Figure 1 - Schematic of initial solidification near meniscus

Other depressions are not related directly to oscillation. A depression characterized by a double skin, with a carburized outer layer, has been reported by Kusano et al. [5] This defect was attributed to carbon pickup by the steel touching the powder flux layer directly and forming a lower melting point steel that ran over the meniscus during level fluctuations. Jenkins et al [6] have shown that another kind of depression may form during the peaks in large, slowly cycling mold level, possibly due to interaction of the newly solidifying shell with the slag rim. Depressions or "laps" in high carbon steel billets have been shown to originate near the meniscus. [7] They were attributed to boiling of the lubricating oil, bleeding through partial tears of the weak shell, and liquid level fluctuations. [7] A different type of surface depression may form longitudinally along the off-corner region of the slab wideface. These have been shown to originate due to inadequate shell growth in the affected region, compression of the shell by excessive taper in the lower part of the mold, and bulging between rolls just below the mold. [8]

Finally, large, random surface depressions, or "ripple marks", have been observed which can extend to depths exceeding 1 mm, especially in steels with carbon content near 0.1%. [4, 9] These depressions have been attributed to thermal stresses due to the large shrinkage of the delta ferrite to austenite phase transformation of these steels. In addition, the peritectic phase transformation favors a high coherency temperature near the equilibrium solidus temperature, and a relatively strong shell. [10] Other grades, particularly steels with higher carbon contents, exhibit segregation, particularly of sulfur and phosphorus. This creates liquid films at the grain boundaries, which persist to much lower temperatures, leading to a coherency temperature far below the equilibrium solidus temperature and a relatively weak shell for a given amount of heat extraction. [10] The weaker shells presumably flatten due to ferrostatic pressure, so are less prone to depressions.

Many previous studies have correlated surface defects, including shallow surface depressions and longitudinal cracks, with fluctuations in the level of the liquid steel meniscus at the top surface of the mold. For example, a study of twin roll casting of stainless steel strip found that shallow surface depressions and longitudinal cracks were both suppressed by taking measures to minimize liquid level fluctuations. [11]

Longitudinal surface cracks often exhibit similar symptoms and are attributed to similar causes as

surface ripple depressions. They are both particularly severe in 0.1% C steels. They are also associated with large variations in mold temperature with time. [12] Longitudinal cracks have been found to depend on factors influencing mold flow conditions, such as the nozzle geometry and submergence depth. [12, 13] This is believed to be due to their increasing likelihood with higher amplitude surface waves. [13]

To alleviate longitudinal cracking, it has been proposed that heat flux from the shell to the mold be reduced at the meniscus. [14] Wolf suggests that transverse depressions in 0.1 %C steels and certain stainless steels also are lessened by avoiding local overcooling near the meniscus, which causes contraction due to a "plastic hinge effect" and rebending. [15] They can be reduced by lowering heat flux, via higher casting speed, higher superheat and an optimized mold flux. Specifically, depressions are found to lessen in 0.1% C steels when using a high melting point, low viscosity flux. [16]

Clearly, the phenomena which occur during the initial stages of initial solidification in the mold of a continuous casting machine are extremely complex. Despite the body of empirical evidence pointing to the importance of initial shell deformation and mold level variations on surface depressions and cracks, very few previous attempts have been made to quantify and understand these phenomena using mathematical models.

One of the few previous studies used the MARC finite element program to predict the deformed shape of the initial shell during an oscillation cycle due to pressure variation in the flux channel. [17] The results agreed qualitatively with some observed trends of oscillation marks, but disagreed with others and differed by an order of magnitude with measured depression depths. No previous deformation model has studied the effect of mold level variations.

Finite-element models of heat transfer and stress have been developed to simulate the transient, two-dimensional temperature, shape, and stress distributions in the solidifying steel shell. [18] In this work, these models are applied to examine temperature and stress development during a brief, but severe fluctuation in liquid level at the meniscus. The results reveal a mechanism by which level fluctuations can lead to surface depressions and cracks.

Model description.

A transient, thermal-elastic-viscoplastic finite-element model, CON2D, [18] has been developed to follow the thermal and mechanical behavior of a section of the solidifying steel shell, as it moves down the mold at the casting speed. It is applied in this work to simulate behavior of a longitudinal slice down the centerline of the wide face shell near the meniscus.

The heat flow model solves the 2-D transient energy equation, using a fixed Lagrangian grid of 3-node triangles. The effects of solidification and solid-state phase transformation on the heat flow are incorporated through temperature-dependent enthalpy and thermal conductivity functions.

The stress model solves for the stresses, strains, and displacements, by interpolating the previously-calculated thermal loads onto a fixed-grid finite-element mesh of 6-node triangles. [18-20] The effects of volume changes due to temperature changes and phase transformation are incorporated through a temperature- dependent thermal-linear-expansion (TLE) function.

The out-of-plane (y-direction) stress is characterized by the state of generalized plane strain. This allows the 2-D model to reasonably estimate the complete 3-D stress state, for the wide, thin shell of interest. This is the best assumption in the absence of friction, because a longitudinal slice down midface of the mold is constrained by the rest of the shell to remain planar as it moves down the mold.

Constitutive behavior for solidifying plain-carbon steel was simulated using the rate-dependent, elastic-viscoplastic model III of Kozlowski. [21] This model was developed to match tensile test measurements of Wray [22] and creep data of Suzuki [23] over a range of strain rates, temperatures, and carbon contents to simulate austenite under continuous casting conditions.

These equations should be extended to properly model the enhanced creep rate in delta ferrite. The elastic modulus varied with temperature (800 ˚C to solidus) according to the following polynomial, based roughly on measured data from Mizukami et al [24]:

$$E\ (GPa) = 674 - 1.53\ T(^{\circ}C) + 0.0012\ T(^{\circ}C)^2 - 0.000000317\ T(^{\circ}C)^3 \qquad (1)$$

These constitutive equations are integrated using a new two-level algorithm, which alternates between solutions at the local node point and the global system equations. [25] Liquid elements, defined by the specified coherency temperature, are set to have no elastic strain. Validation of this model using both analytical solutions and measurements from operating slab casters are described elsewhere. [26]

Boundary Conditions

A Lagrangian formulation is adopted, so the model domain is initially assumed to contain stress-free liquid at uniform temperature, T_o. The shell is assumed to form continuously below a sharp meniscus and move downward at the casting speed, as illustrated in Figure 2. Thus, the heat flow model imposes a zero heat flux condition on those portions of the mesh above the liquid level prior to the level drop.

$$q = 0, \qquad \text{for } z > V_c\, t \text{ and } x = 0. \qquad (2)$$

$$q = h_c\,(T - T_m), \qquad \text{for } z < V_c\, t \text{ and } x = 0. \qquad (3)$$

After the shell has moved downward 20 mm (1.2s), the liquid level is suddenly dropped for 0.6s. This roughly approximates the duration of an oscillation cycle or random flow transient. During this time, liquid elements are ignored and the following boundary condition is imposed along the exposed solid shell, defined by the location of the solidus isotherm at the time of the level drop:

$$q = h_a\,(T - T_a), \qquad \text{for } 1.2s < t < 1.8s. \qquad (4)$$

Finally, the level is raised again at 1.8s, by restoring the liquid elements at the initial temperature, and allowing solidification to continue. Note that the level is restored only to the top of the shell tip, so that overflow of the meniscus is not simulated. Heat transfer coefficients and temperatures are given in Table I. Zero heat flux is assumed across the top, bottom, and liquid-steel sides of the domain.

All external surface tractions were set equal to zero, except for fixing three nodal displacements at the domain bottom to prevent rigid body motion. This stress-free condition models shell behavior in the absence of mold friction, pressure in the flux channel, or ferrostatic pressure.

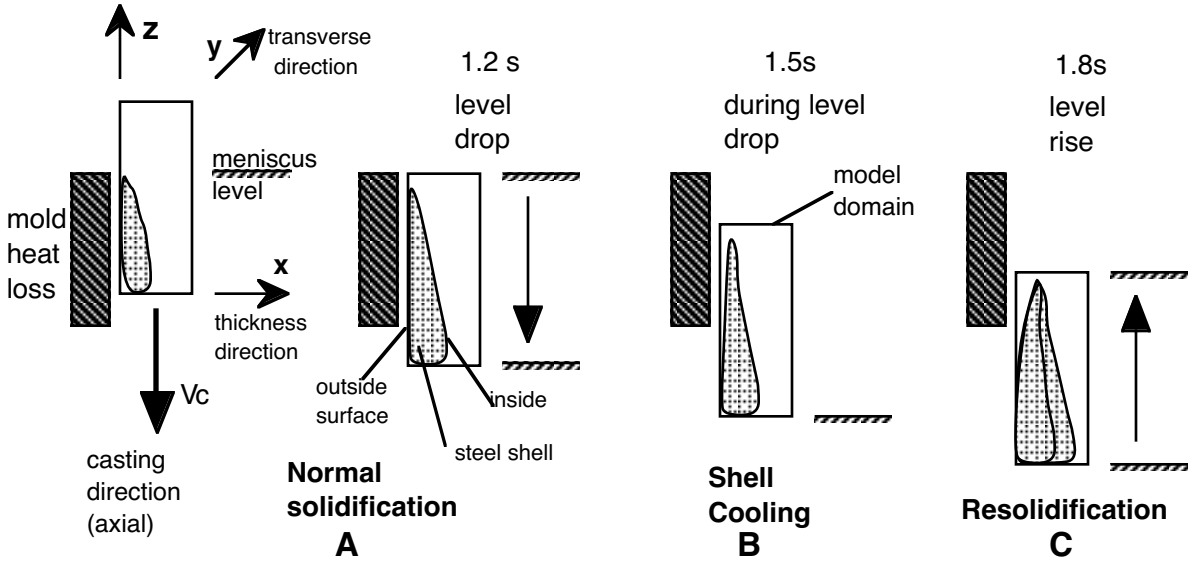

Figure 2 - Movement of longitudinal slice model domain during simulation

Table I. Simulation Conditions

Material properties		Ultra-low carbon steel (ULC)
	Composition	0.003%C
	Liquidus Temperature	1535.76 ˚C
	Solidus Temperature	1534.63 ˚C
Casting Conditions		
T_o	Initial temperature	1537 ˚C
	Superheat	1.24 ˚C
V_c	Casting speed	16.7 mm/s (1 m/min)
T_m	Mold temperature	250 ˚C
h_c	Mold / shell heat transfer coefficient	2000 W/m^{2}K
	Mold friction	none
Level fluctuation conditions		
	duration	0.6 s
	Distance of level drop	30 mm
	Distance of subsequent level rise	20 mm
T_a	Ambient temperature	35 ˚C
h_a	Ambient heat transfer coefficient	272 or 200 W/m^{2}K
Simulation conditions		
	Domain size	3 x 20 mm
	Stress state	generalized plane strain

Discussion of Model Assumptions

Ultra-low carbon steel (0.003%C) was selected for this initial work for several reasons. First, this alloy is almost pure iron, so exhibits very little segregation. Thus, the mushy zone (between solidus and liquidus temperature) is very thin and the coherency temperature (at which the shell can bear a load) is assumed equal to the solidus temperature. This simplifies development of the model considerably. Secondly, the high coherency temperature of this alloy is expected to make it behave in a similar manner to the 0.1 %C peritectic steels. Finally, ultra-low carbon steel is commercially important in its own right.

The model neglects pressure forces which act on the shell. This includes ferrostatic pressure, which tends to flatten out the distorted shell when the level is high. The model also ignores pressure variations in the molten flux, which tend to enhance bending of the shell towards the liquid, which is one of the causes of oscillation marks. These pressures are both on the order of 1 kPa. To include them properly requires a transient flow analysis of both the molten flux and the molten steel. Although these effects are important, they are not expected to completely overshadow thermal distortion of the shell, if it has a fully solid layer.

The model ignores the drop in heat transfer that should occur when the shell loses contact with the mold and bends towards the liquid. Including this coupled phenomenon would increase surface temperature and lead to even more bending toward the liquid than predicted.

The model ignores the curvature of the meniscus and further assumes zero heat flow above the meniscus. It also ignores nonuniform dissipation of superheat due to flow in the liquid pool. This means that meniscus solidification cannot be modeled. Including this effect would presumably allow prediction of the shape of subsurface hooks and oscillation marks.

Relatively slow heat transfer is assumed, representing conditions for an optimal mold powder for depression-sensitive grades, with good coverage and lubrication in the meniscus region. Thus, defects caused by nonuniform heat flow are not simulated. Nucleation undercooling effects are also ignored.

The model neglects mold friction. Sticking of the shell to the mold naturally would generate tensile stress, which may contribute to cracks. For example, sticking of the shell to the mold on either side of a longitudinal depression would concentrate strain at the hottest, weakest portion of the shell. This is another likely mechanism contributing to longitudinal cracks.

Slag entrainment during the level drop was ignored. In addition to creating subsurface inclusion defects, this would slow down resolidification after the level rises. The results presented here show very fast solidification due to the perfect contact assumed between the liquid and shell after the level rise.

The model ensures no elastic strain in the liquid, so thermal stress and distortion are generated only by thermal contraction in the solid state. Strain on the liquid is assumed to generate fluid flow, as necessary. For high coherency-temperature materials, such as considered in this work, this assumption is probably reasonable. In regions of high solid fraction in grades with dense columnar mushy zones, it might not be.

Results

Two simulations were performed. The first considers thermal stress development in a section of solidifying shell that is fully constrained from thermal distortion. Figure 3 shows the temperature profile across the shell at three important times before, during, and after the sudden 0.6s drop in liquid surface level. A portion of the shell 20 mm below the meniscus at the time of the level drop is considered. Figure 4 shows the corresponding axial (z) stress distributions through the shell. Calculated nodal values, shown as points in this figure, show oscillation due to the course mesh, so a smooth curve is drawn through each set. Because there is no external stress, such as mold friction, the stress profiles across the shell must average zero to maintain equilibrium, so the tensile and compression regions must balance. Finally, note that stress must decrease to zero at the solid / liquid interface, as defined by the coherency temperature (assumed to be the solidus). This is required because liquid always solidifies stress-free.

The second simulation allows completely free bending of the shell. Temperature contours within this shell are shown in Figure 5, superimposed on the distorted shape, which is magnified two times. The computed axial stresses are negligible, having been replaced by bending of the shell. Stresses through the thickness (x direction) are also negligible. However, Figure 6 shows the maximum transverse (y) stress distribution along the surface, with the corresponding temperature profile, which occurs at the end of the level drop. These results are discussed together in chronological order.

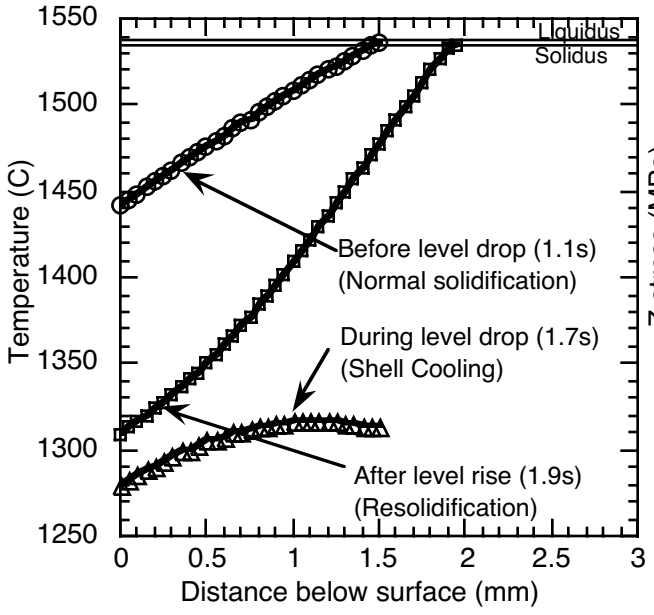

Figure 3 - Temperature profile through shell

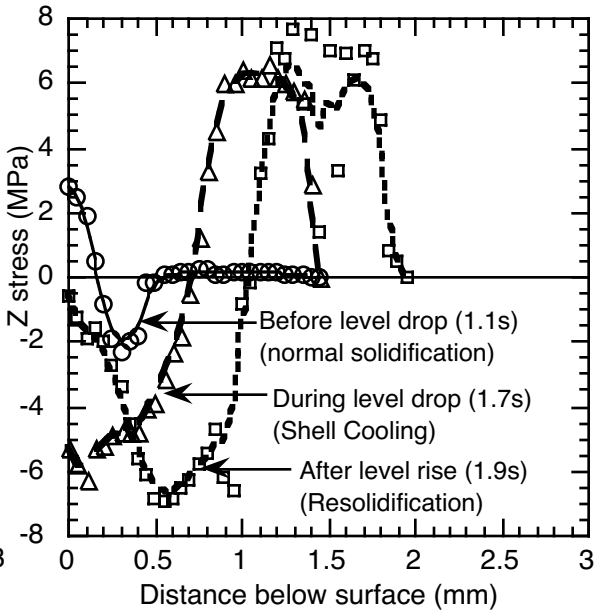

Figure 4 - Axial (z) stress profiles through constrained shell

A. During solidification

The nature of both the stress distribution and corresponding shape of the solidifying shell depends on the cooling history, as defined by the heat transfer coefficient, h_c, on the boundary of the shell facing the mold. Figures 3 and 5 a) show the temperature distribution during the initial stages of uniform solidification near the meniscus. Relatively high temperature gradients exist through the shell thickness, as the shell surface is cooling rapidly.

When the cooling rate is high after initial solidification, a significant temperature gradient is also created in the casting direction (z). Thus, the shell surface cools and contracts rapidly. When constrained, this generates a slight z-tensile stress within the surface layer of the shell, balanced by slight compression beneath it. Stresses during solidification are low, on the order of only 2 MPa, due to the rapid creep relaxation and low elastic modulus at these high temperatures. The predicted stress levels are consistent with flow stress measurements of 1 - 5 MPa, made on solidifying shells by Hiebler et al. [27]

When unconstrained, these z-stresses cause the shell to bend slightly in a concave shape toward the mold walls. This is illustrated in Figure 5a). The depth of the depression is very small however, being less than 0.1 mm over the 20 mm length of shell simulated. The remaining z-stresses are still tensile at the surface and compressive in the subsurface. However, their magnitude is almost negligible, due to the rapid stress relaxation at these high temperatures.

These results contrast with conditions later during solidification, when the surface cooling rate is slow. In this case, reported elsewhere, [25] the surface temperature becomes relatively uniform. Then subsurface cooling and contraction generates subsurface tension, which induces compression at the surface of the shell. This tends to reverse the slight bending of the shell from the mold, presenting a slightly convex shape toward the mold walls instead.

B. During drop in level

Figure 3 shows that temperature throughout the shell tip decreases rapidly during the short 0.6s level drop, falling about 200 ˚C even 20 mm below the meniscus. Without the heat supplied from the molten metal, the mold is able to extract sensible heat from the thin shell very quickly, even with the relatively small heat transfer coefficient assumed in this work.

Temperature gradients across the shell thickness disappear also, as temperature within the thin shell equilibrates. This means that the shell inside cools more than the outside. This is naturally accompanied by a greater contraction of the inside of the shell, relative to the outside surface. When constrained, this generates large subsurface tensile stresses, (6 MPa) seen in Figure 4. Corresponding compression stresses are generated at the surface.

When unconstrained, this internal contraction causes the shell to bend significantly toward the liquid, leaving a convex shape facing the mold. This contraction is calculated to reach 0.45 mm over the 20 mm length of shell modeled, as shown in Figure 5 b). This prediction appears roughly consistent with the measured shape of 5 mm high, ultra-low carbon and peritectic steel droplets quenched on a copper chill [28]. These researchers observed bending which produced a concave shape toward the mold and gaps of 0.2 mm over a length of 8 mm.

Equally important to the large distortion of the shell toward the liquid are the stresses generated. Stress levels in the shell thickness (x) and casting directions (z) remain very low. However, Figure 6 shows that the calculated y-stress along the shell surface reaches a maximum of over 40 MPa at the end of the level drop. This is caused by the large axial temperature gradient combined with constraint by the rest of the wide face shell. Naturally, the average stress is zero, due to the assumption of no friction. The shell tip is compressive due to the δ to γ volume expansion. However, just below the tip, thermal contraction is relatively large. This creates high tensile stress across the entire shell over an axial distance of 6mm for this 20mm level drop.

These high tensile stresses are consistent with viscoplastic deformation at these low temperatures. However, in crack-sensitive peritectic grades, this might be sufficient to generate longitudinal surface cracks.

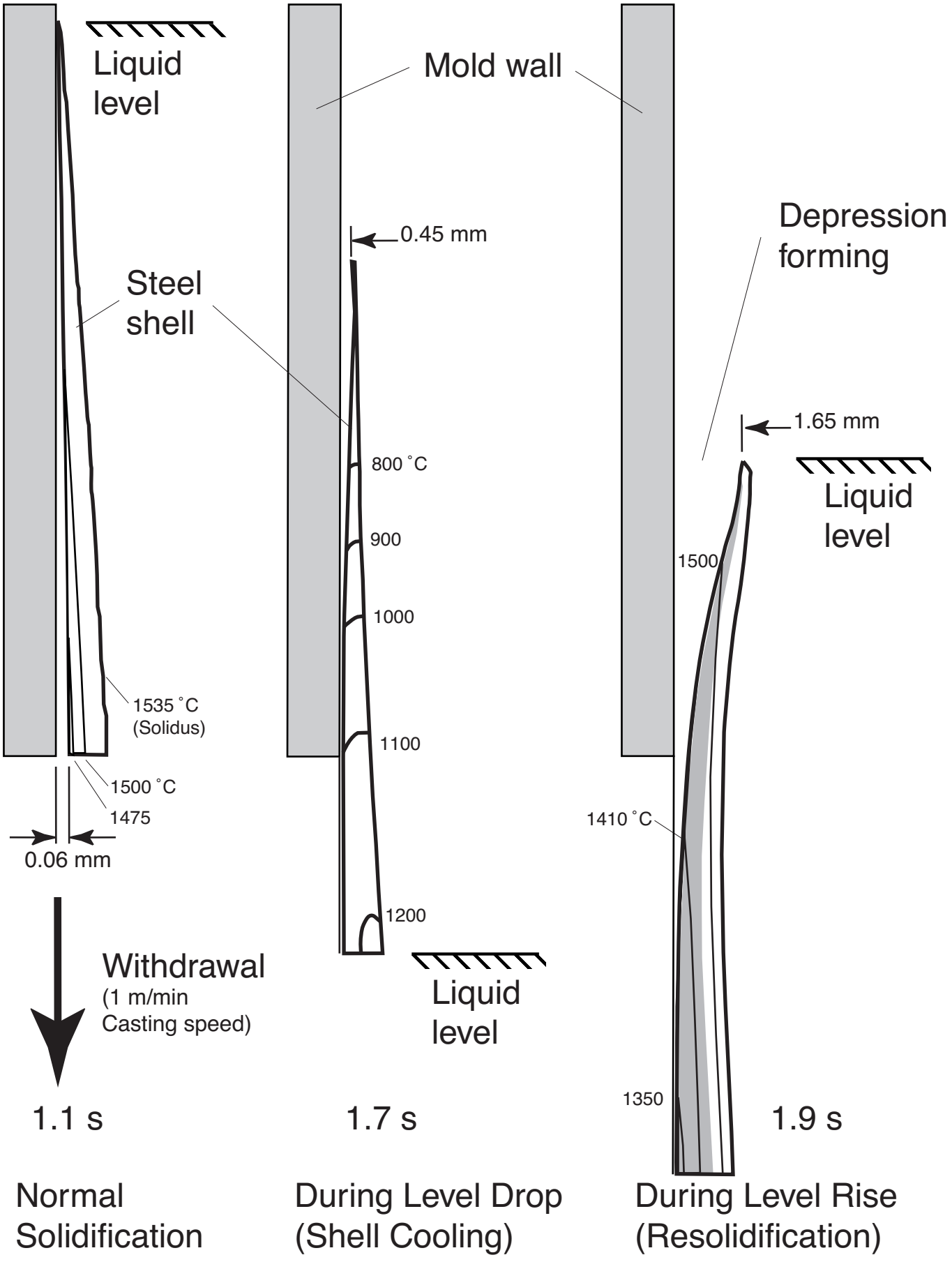

Figure 5 - Distorted shell shape with temperature contours (˚C)

C. After rise in level

Figures 3 and 5 c) show the rapid increase in temperature, shell thickness, and distortion which is predicted to occur after the liquid level is suddenly raised back up to the tip of the shell. Reestablishing contact with the liquid causes solidification to continue, generating a "newly solidified" shell on top of the existing solid shell. The initial rate of the new solidification is rapid because perfect contact is assumed between the liquid steel and the existing shell. This new solidification quickly heats the inside of the existing shell, restoring the high temperature gradient through the shell typical of normal solidification (Figure 5a).

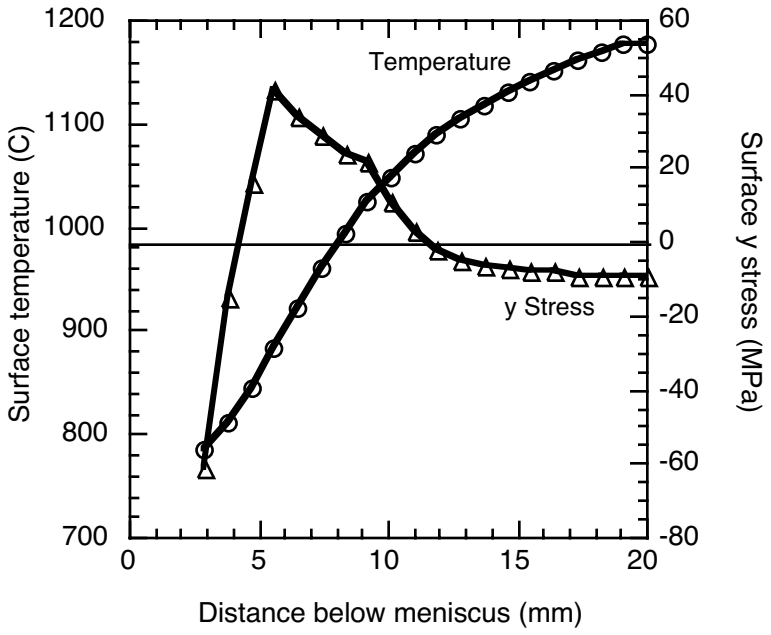

Figure 6 - Y stress and temperature down shell surface (1.8s)

The increased average temperature of the older solidified layer causes it to expand. However, the newly solidified layer restrains this expansion, if it is of sufficient strength, which is the case for the ultra-low steel layer studied here. Moreover, this newly solidified layer itself is cooling and contracting. Unlike initial solidification against the mold, this new layer is unable to contract free of stress and distortion during its initial cooling stages. The result is further bending of the shell towards the liquid. The increase in tip distortion is significant, reaching 1.65 mm, as illustrated in Figure 5 c).

Mechanism of Surface Depressions and Longitudinal Cracks

The results presented in the previous section illustrate a detailed mechanism to form shallow surface depressions and short longitudinal cracks due to a sudden level fluctuation. First, a severe drop in liquid level at the meniscus causes bending of the shell away from the mold toward the liquid. The subsequent rise in liquid level increases this bending. Finally, overflowing of the shell tip after the level rise begins creation of a new shell closer to the mold wall. This leaves behind a surface depression to travel down the mold.

Deeper and longer level drops obviously should create deeper depressions. The location of the depressions should naturally concentrate at locations on the strand perimeter where level fluctuations are frequent. Due to the random nature of level fluctuations, these depressions should occur randomly, with irregular but generally transverse shapes. They may also have oxides beneath the outer layer of steel, if the level drop entraps liquid mold flux.

A severe level drop also causes rapid cooling of the shell tip and high transverse stresses. These stresses could generate longitudinal cracks along the shell tip, if the steel grade is susceptible. These cracks are predicted to be shallow, longitudinal surface cracks, less than 1 mm deep and 5-10 mm long, depending on the extent of the level fluctuation.

Discussion

This work shows how meniscus level fluctuations can directly initiate a particular type of transverse surface depression and / or short, shallow longitudinal surface cracks, by generating thermal distortion and stress in the initial shell. This mechanism complements other mechanisms involving indirect effects of mold level changes on defects, such as disrupting the uniform feeding of lubricating flux into the mold / shell gap.

These defects initiated by level changes can be aggravated later by other mechanisms. For example, as each transverse depression moves down the mold, it causes a local reduction in the heat transfer rate beneath it, especially if there was a lubrication problem leading to a local air gap. This produces a drop in mold temperature which is delayed by the casting speed and distance below the meniscus. This is consistent with the strong statistical correlation between mold level fluctuations and mold temperature fluctuations that has been observed experimentally. [29] Furthermore, solidification at the reduced cooling rate should produce a courser dendrite arm spacing beneath each depression. The hotter shell beneath each depression is weaker, so any additional tensile stress, such as generated by mold friction due to a lack of lubrication, would be expected to concentrate at the existing longitudinal surface crack, propagating it longer and deeper, possibly connecting with subsurface cracks. [30] The tensile stress also encourages macrosegregation of interdendritic liquid toward the surface, further weakening the shell and enabling crack growth.

The bending mechanism shown in this work is expected to produce the deepest depressions in solidifying shell tips that have the highest solid-state contraction and the highest coherency temperature relative to the surface temperature. This may explain the observed effect of steel grade on ripple mark depression susceptibility. The mechanism has been modeled here only for ultra-low carbon steel. Solidifying shell tips of this pure metal have a high coherency temperature, owing to their narrow mushy zone and lack of segregation.

It is suspected that steels near 0.1% C should also be prone to the proposed bending mechanism, for reasons explained by Wolf. [10] First, these peritectic steels experience the most solid state thermal and phase transformation contraction. Second, peritectic steels also exhibit a high coherency temperature, only slightly below the equilibrium solidus temperature. Finally, these steels also experience interdendritic weakness, making them more prone to cracks than the ultra-low carbon steel.

Steels with a wide mushy zone and segregation, such as high carbon steels, are likely not susceptible to this depression mechanism. This is because these steels retain a liquid fraction at the surface for distances down the mold far greater than the maximum likely liquid level fluctuation. With the complete shell above the coherency temperature, bending strain cannot develop.

The bending mechanism shown here might contribute to the formation of deep oscillation marks. At any time during the oscillation cycle, if the surface level dropped to expose the shell tip, then the predicted bending of the shell away from the mold would amplify the depth of that oscillation mark. This might help to explain why peritectic steel grades tend, on average, to have deeper oscillation marks [16] than other steel grades. It also predicts that deep oscillation marks are more likely at positions around the mold perimeter where level fluctuations are most frequent.

The bending mechanism shown here is not expected to explain the shape of subsurface “hooks”, caused by meniscus freezing. Indeed, these hooks have more curvature than the gradual depressions calculated in this work. This is because these “hooks” take their shape from the original curved liquid meniscus, which is controlled by surface tension balanced with gravity, dynamic forces in the liquid and pressure in the flux channel. These phenomena were not modeled in the present work.

The obvious practical implication of this work is that severe, sudden drops in meniscus level are detrimental to surface quality, even with an optimal flux practice, adequate lubrication, and otherwise uniform conditions. Thus, measures should be taken to control meniscus level in the mold to avoid these fluctuations. This involves careful choice of nozzle geometry, argon injection practice, and other casting conditions affecting liquid steel flow near the meniscus.

Conclusions

Two-dimensional, transient finite-element model simulations have shown how a sudden drop in liquid level affects temperature gradients, thermal distortion, and stress distribution in the solidifying steel shell near the meniscus.

1) These results illustrate an important mechanism assisting the formation of surface depressions and longitudinal cracks at the meniscus.

2) A sudden level drop induces significant thermal distortion of the shell towards to liquid. The subsequent rise in liquid level causes the shell to bend even further inward. Shell distortion greater than 1 mm is predicted for a 0.6s level fluctuation of 20 mm. Subsequent overflow of the bent shell would create a transverse surface depression.

3) Large, rapid level drops induce large axial temperature gradients, which create high transverse tensile stresses in the shell, even in the absence of mold friction. This may be a cause of short, shallow, longitudinal surface cracks.

4) Ultra-low carbon steels and peritectic steels are expected to be particularly prone to this mechanism, owing to their high coherency temperature, which leads to strong initial shells that can resist flattening by ferrostatic pressure.

This mechanism emphasizes the vital importance of controlling mold level in order to avoid surface depressions, longitudinal cracks, and other defects.

Acknowledgments

The authors wish to thank AK Steel, (Middletown, OH), Allegheny Ludlum, (Brackenridge, PA), Armco Inc. (Middletown, OH), Inland Steel Corp. (East Chicago, IN), LTV (Cleveland, OH), and BHP Co. Ltd. (Melbourne, Australia) for their continued support of our research and the National Center for Supercomputing Applications (NCSA) at the University of Illinois for computing time.

References

1. E. Takeuchi and J.K. Brimacombe, "The formation of oscillation marks in the continuous casting of steel slabs," Metallurgical Transactions B, 15B (Sept) (1984), 493-509.
2. R.B. Mahapatra, J.K. Brimacombe and I.V. Samarasekera, "Mold Behavior and its Influence on Product Quality in the Continuous Casting of Slabs: Part II. Mold Heat Transfer, Mold Flux Behavior, Formation of Oscillation Marks, Longitudinal Off-corner Depressions, and Subsurface Cracks," Metall. Trans. B, 22B (December) (1991), 875-888.
3. I.V. Samarasekera, J.K. Brimacombe and R. Bommaraju, "Mold Behavior and Solidification in the Continuous Casting of Steel Billets," Transactions of Iron and Steel Society, 5 (1984), 79-93.
4. I.G. Saucedo, "Early Solidification during the Continuous Casting of Steel," in Mold Operation for Quality and Productivity, (Warrendale, PA: Iron and Steel Society, 1992), 43-53.
5. A. Kusano et. al., "Improvement of Mold Fluxes for Stainless and Titanium Bearing Steels," in Steelmaking Conference Proceedings, 74, (Warrendale, PA: Iron and Steel Society, 1991), 147-151.
6. M.S. Jenkins et. al., "Investigation of Strand Surface Defects using Mold Instrumentation and Modelling," in Steelmaking Conference Proceedings, 77, (Warrendale, PA: Iron and Steel Society, 1994), 337-345.
7. S. Kumar et. al., "Chaos at the Meniscus - the Genesis of Defects in Continuously Cast Steel Billets," in PTD Conference Proceedings, 13, (Warrendale, PA: Iron and Steel Society, 1995), 119-141.
8. B.G. Thomas, A. Moitra and R. McDavid, "Simulation of Longitudinal Off-Corner Depressions in Continuously-Cast Steel Slabs," in PTD Conference Proceedings, 13, (Warrendale, PA: Iron and Steel Society, 1995), 143-156.

9. S.N. Singh and K.E. Blazek, "Heat Transfer and Skin Formation in a Continuous Casting Mold as a Function of Steel Carbon Content," in Open Hearth Proceedings, 57, (Warrendale, PA: Iron and Steel Society, 1974), 16-36.
10. M. Wolf and W. Kurz, "The Effect of Carbon Content on Solidification of Steel in the Continuous Casting Mold," Metallurgical Transactions B, 12B (3) (1981), 85-93.
11. H. Yasunaka et. al., "Surface Quality of Stainless Steel Type 304 Cast by Twin-roll Type Strip Caster," Iron & Steel Institute of Japan, 35 (6) (1995), 784-789.
12. S.G. Thornton and N.S. Hunter, "The Application of Mould Thermal Monitoring to Aid Process and Quality Control When Slab Casting for Heavy Plate and Strip Grades," in Steelmaking Conference Proceedings, 73, (Warrendale, PA: Iron and Steel Society, 1990), 261-274.
13. E. Hoffken, H. Laz and G. Pietzko, "Development of Improved Immersion Nozzles for Continuous Slab Casting," in Proceedings of the 4th International Conference Continuous Casting, (Brussels: Stahl & Eissen, 1988), 461-473.
14. K. Nakai et. al., "Improvement of Surface Quality of Continuously Cast Slab by Reducing Heat Flux Density in Mould," in Continuous Casting '85 Proceedings, (London, UK: Institute of Metals, 1985), paper 71.
15. M. Wolf, "Strand Surface Quality of Austenitic Steels: Part I. Macroscopic Shell Growth and Ferrite Distribution," 13 (5) (1986), 248-257.
16. M.M. Wolf, "Mold Heat Transfer and Lubrication Control - Two Major Functions of Caster Productivity and Quality Assurance," in PTD Conference Proceedings, 13, (Warrendale, PA: Iron and Steel Society, 1995), 99-117.
17. S. Takeuchi et. al., "Control of Oscillation Mark Formation during Continuous Casting," in Mold Operation for Quality and Productivity, (Warrendale, PA: Iron and Steel Society, 1992), 37-41.
18. A. Moitra, "Thermo-mechanical model of Steel Shell Behavior in Continuous Casting" (Ph.D. Thesis, University of Illinois at Urbana-Champaign, 1993).
19. A. Moitra and B.G. Thomas, "Application of a Thermo-Mechanical Finite Element Model of Steel Shell Behavior in the Continuous Slab Casting Mold," in Steelmaking Proceedings, 76, Iron and Steel Society, 1993), 657-667.
20. B.G. Thomas and H. Zhu, "Evaluation of Finite Element Methods for Simulation of Stresses During Solidification" (Paper presented at World Conference on Computational Mechanics III, Chiba, Japan, 1994).
21. P. Kozlowski et. al., "Simple Constitutive Equations for Steel at High Temperature," Metallurgical Transactions A, 23A (March) (1992), 903-918.
22. P.J. Wray, "Effect of Carbon Content on the Plastic Flow of Plain Carbon Steels at Elevated Temperatures," Metallurgical Transactions A, 13A (1) (1982), 125-134.
23. T. Suzuki et. al., "Creep Properties of Steel at Continuous Casting Temperatures," Ironmaking and Steelmaking, 15 (2) (1988), 90-100.
24. H. Mizukami, K. Murakami and Y. Miyashita, "Mechanical Properties of Continuously Cast Steels at High Temperatures," Nihan Kokan Corporation, Tetsu-to-Hagane (Iron and Steel), 63 (146) (1977), S 652.
25. H. Zhu and B.G. Thomas, "Evaluation of Finite Element Methods for Simulation of Stresses During Solidification" (Report, University of Illinois, 1994).
26. B.G. Thomas, A. Moitra and H. Zhu, "Coupled Thermo-mechanical Model of Solidifying Steel Shell Applied to Depression Defects in Continuous-cast Slabs," in Modeling of Casting, Welding and Advanced Solidification Processes VII, 7, M. Cross and J. Campbell, eds., (Warrendale, PA: TMS, 1995), 241-248.
27. H. Hiebler et. al., "Inner Crack Formation in Continuous Casting: Stress or Strain Criterion," in Steelmaking Conference Proceedings, 77, (Warrendale, PA: Iron and Steel Society, 1994), 405-416.
28. S. Dong, E. Niyama and K. Anzai, "Free Deformation of Initial Solid Shell of Fe-C Alloys," Iron & Steel Inst. of Japan, 35 (6) (1995), 730-736.
29. J. Suni and H. Henein, "Analysis of Shell Thickness Irregularity in Continuously Cast Middle Carbon Steel Slabs Using Mold Thermocouple Data," Steelmaking Conference Proceedings, 76 (1993), 331-336.
30. J.K. Brimacombe, F. Weinberg and E.B. Hawbolt, "Formation of Longitudinal, Midface Cracks in Continuously-Cast Slabs," Metallurgical Transactions B, 10B (1979), 279-292.